



Published in final edited form as:

J Biomed Mater Res A. 2007 June 15; 81(4): 939–947.

Selective cell proliferation can be controlled with CPC particle coatings

J.A. Szivek^{1,2}, D.S. Margolis¹, A.B. Schnepf¹, W.A. Grana¹, and S.K. Williams²

¹*Orthopaedic Research Laboratory, Department of Orthopaedic Surgery, University of Arizona, Tucson, Arizona*

²*Biomedical Engineering Program, University of Arizona, Tucson, Arizona*

Abstract

To develop implantable, engineered, cartilage constructs supported by a scaffold, techniques to encourage rapid tissue growth into, and on the scaffold are essential. Preliminary studies indicated that human endothelial cells proliferated at different rates on different calcium phosphate ceramic (CPC) particles. Judicious selection of particles may encourage specific cell proliferation, leading to an ordered growth of tissues for angiogenesis, osteogenesis, and chondrogenesis. The goal of this study was to identify CPC surfaces that encourage bone and vascular cell growth, and other surfaces that support chondrocyte growth while inhibiting proliferation of vascular cells. Differences in bone and vascular cell proliferation were observed when using epoxy without embedded CPCs to encourage bone cells, and when three CPCs were tested, which encouraged vascular cell proliferation. One of these (CPC 7) also substantially depressed cartilage cell proliferation. Only one small-diameter crystalline CPC (CPC 2) supported rapid chondrocyte proliferation, and maintained the cartilage cell phenotype.

Keywords

chondrocytes; osteoblasts; endothelial cells; hydroxyapatite; proteoglycan

INTRODUCTION

Osteoarthritis now affects over 20 million Americans with similar numbers reporting pain and disability from knee injuries.¹ Currently there are no therapies for the treatment of large focal lesions (larger than 2 cm) in the articular surface of the knee to restore the joint to its original condition.^{2–4} While total knee arthroplasty is a widely utilized treatment for excessive joint pain in arthritis patients, it requires extensive bone resection and cannot restore normal proprioception.⁵ In addition total joints can loosen and wear out in patients who are physically active.^{6,7} Engineered tissue constructs and repair of cartilage could provide an alternative for active patients with large cartilage defects and extensive arthritic changes.^{8–10} This approach will preclude the need for massive bone resection and concomitant problems associated with artificial joint replacements.

A long history of failed attempts to induce growth and complete repair of a replacement cartilage layer *in situ* using a variety of techniques³ suggests that techniques involving the engineering of a cartilage tissue on a scaffold *in vitro* must be explored.^{3,4} Success of an engineered cartilage construct on a scaffold will depend not only on growth of the cartilage itself but on rapid fixation of the supporting scaffold in surrounding tissue by utilizing scaffold

materials with the appropriate surface chemistry^{11–13} and scaffold constructs with a specific surface structure^{14–16} and porosity.^{17,18} Judicious selection of scaffold coatings¹⁹ and substrates are expected to selectively encourage various cells²⁰ and tissue to form in specific scaffold locations, leading to an ordered growth of tissues containing selected paths for angiogenesis, osteogenesis, and chondrogenesis.

Preliminary studies using rat cells have indicated that different proliferation rates could be induced on different calcium phosphate ceramic (CPC) particle surfaces.²⁰ The goal of this study was to compare proliferation rates of cells from three primary cell lines (microvascular endothelial cells, bone derived cells, and cartilage derived cells) collected from the same test animal, on various CPC surfaces to develop a strategy to encourage the growth of a specific cell type, and consequently tissue type, into a specific region of a scaffold. It is hypothesized that CPC particles that encourage rapid cartilage cell proliferation will not encourage rapid microvascular endothelial cell and bone cell proliferation and that surfaces that encourage rapid microvascular endothelial cell and bone cell proliferation will not encourage rapid cartilage cell proliferation.

MATERIALS AND METHODS

CPC characterization and preparation

Six types of CPC particles were used in this study. Five of the particles were identified as CPCs 1, 2, 3, 6, and 7 and had previously been characterized and evaluated for their *in vivo* bone bonding characteristics.²¹ The sixth particle type tested, CPC 14, was characterized according to size, shape, and degree of crystallinity using scanning electron microscopy and X-ray diffraction (XRD) analysis to allow comparison with the characteristics of the other five CPCs (Table I).

For each experiment 42 of the wells in the 48-well flat-bottomed tissue culture plates (Becton Dickinson, Franklin Lakes, NJ) were coated with 14 μ L of Master Bond EP42H epoxy (Master Bond, Hackensack, NJ). CPC particles were poured into 36 of the epoxy-coated wells (six wells of each type of CPC) immediately after mixing and application of the epoxy. After 12 h, nonadherent CPC particles were removed by inverting the plate and using a blast of compressed air. Plates were gas sterilized using ethylene oxide and aerated for 4 h. Experimental wells were presoaked with 0.2 mL/well of media specific to each cell type for one hour prior to cell seeding.

Representative CPC-coated well plates prepared in the same way as those to be used for cell culture studies were sectioned through the center of each well. A total of six wells with each CPC coating, as well as six epoxy coated wells, and six uncoated wells were analyzed. Digital images of the well plates were collected at 35 \times magnification under fluorescent light using a M3Z Wild microscope (Heerbrugg, Switzerland) coupled to a Cool Pix digital camera (Nikon, New York). For each well plate the chord length (measured as the length of the bottom of the well plate) and the length of the CPC-coated surface that the cells were cultured on were measured using Image J. The % surface length of each CPC-coated well plate was calculated using the ratio of these values. The area of each well plate was then calculated using the surface length to determine the bottom surface area and the circumference to assess the area coated along the side walls of the plate.

In addition to calculating the surface area of each type of CPC, the lengths of exposed CPC particles were measured along CPC-coated surface. The relative amount of the CPC-coated surface was calculated using the following formula: % Surface with Exposed CPC = length of exposed CPC/total surface length \times 100%. To facilitate comparison of all surfaces, the cell numbers were normalized for area relative to the control uncoated plates.

Cell culture studies

The proliferative properties of cells in eight experimental groups were examined. Six sets of wells were used to evaluate each of the eight groups. Each of the six CPC types was tested and two control groups were compared to the six experimental groups. Controls were (1) cells grown in untreated wells (with media only) for comparison to cultures in CPC-coated wells and (2) cells grown in adhesive covered wells to assess the response of cells to the adhesive used to attach particles to the well surfaces.

Three types of cells were extracted from fresh dog carcasses following a protocol approved by the University I.A.C.U.C., in accordance with National Institutes of Health guidelines. The three cell types were harvested from each carcass to evaluate potential variability of the cell response due to genetic variation.

Endothelial cells (MVEC) from falciform fat, were collected utilizing a technique described by Williams et al.²² Briefly, this technique involves use of a midline laparotomy performed to retrieve falciform fat. Fat was then minced and digested in a 50% ratio with digestion media in a 37°C shaker bath for 30 min. Digestion media consisted of 4500 U/mL collagenase I (EMD Biosciences, San Diego, CA) and 8 mg/mL Bovine Serum Albumen (Sigma-Aldrich, St. Louis, MO) dissolved in dication-free phosphate buffered saline (Sigma-Aldrich). Endothelial cells were isolated from the digested fluid by fractional centrifugation for 4 min at 700g. The resulting cell pellet was suspended in M199 medium (Sigma-Aldrich) supplemented with 15% fetal bovine serum (FBS) (HyClone, Logan, UT), 5 mM HEPES (Sigma-Aldrich), and endothelial cell growth supplement,²³ which was then seeded and expanded on 1% gelatin-coated tissue culture plastic.

Cartilage derived cells(CDC) were collected from articular cartilage explants. The chondrocytes in these explants were taken from the surface of the olecranon using a sterile scalpel. Bone derived cells (BDC) were extracted from bone drillings collected from the head of the humerus. A hole created with a sterile 6.35-mm (0.25 inch) surgical drill was used to produce the bone drillings.

Tissue specimens were placed in growth medium and examined daily using a light microscope while CDCs and BDCs grew and migrated out of the tissues. Cells were passed from flasks and expanded in DMEM (Sigma-Aldrich) supplemented with 10% FBS (HyClone), 5 nM HEPES (Sigma-Aldrich), 50 g/mL L-ascorbic acid (Sigma-Aldrich), 100 U/mL penicillin, and 100 g/mL streptomycin (Invitrogen, Carlsbad, CA).

All cells that were used were first or second passage. They were seeded into wells at an initial density of 10,000 cells per square centimeter. MVEC cultures were grown on CPC surfaces for 24 h before cell metabolism was evaluated. The slower growing CDC and BDC cells were cultured for 72 h before they were evaluated.

Assays

Relative cell metabolism was determined as an indicator of relative cell populations, using a Sigma TOX-2 XTT assay kit(Sigma-Aldrich). Cells were incubated for 2 h in the presence of XTT. Mitochondrial action in the cells cleaved the XTT tetrazolium ring and the optical density of the resulting dye was measured at a 450 nm wavelength. Cells were also visualized using light microscopy and quantified by means of digital imaging and cell counting. Results from cell counts were used to calibrate cell estimates determined from XTT studies. MVECs and BDCs were easily visually distinguishable. To insure that CDCs remained viable and retained their phenotype over the course of all experiments, proteoglycan assays were performed on these cells. No proteoglycan assay was performed on BDC or MVEC cultures. Statistical analysis was performed using an ANOVA with a Tukey HSD Post Hoc test.

Media extracted from experimental wells after 2 days of cellular activity was assessed for proteoglycan content using a Dimethyl methylene Blue assay²⁴ adapted for use in 48-well plates. In a 48-well plate, 75 μL of sample was digested for 1 h at 60°C in 40 μL 20 nM Sodium Phosphate (pH 6.8), 1 mM EDTA, 2 mM DTT, and 60 $\mu\text{g}/\text{mL}$ Papain. After incubation, 85 μL of 50 mM Tris buffered HCl (pH 8.0) containing 0.3718 μg iodoacetic acid was added to each sample. For each well, 20 μL of digested sample was transferred to a new well plate containing 280 μL of 16 mg/mL Dimethyl methylene blue reagent dissolved in 63 mM sodium chloride (pH of 3.0). Absorbance was immediately recorded in a plate reader at a wavelength of 520 nm. The proteoglycan content of media samples was measured and evaluated against serial dilutions of a proteoglycan standard from bovine nasal cartilage (Sigma-Aldrich).

RESULTS

CPC characterization

CPC 1 [Fig. 1(a)] and 2 [Fig. 1(b)] were both noted to be crystalline hydroxyapatite (HA) (Table I). Scanning electron microscopy (SEM) showed that CPC 1 was composed of angular medium sized particles. CPC 2 was observed to be composed of rounded particles with a very small particle size. CPC 3 and 6 were relatively amorphous in crystal structure. SEM indicated that CPC 3 [Fig. 1(c)] was comprised of relatively angular medium sized HA particles and CPC 6 [Fig. 1(d)] was composed of fine rounded particles. CPC 6 was the only tricalcium phosphate (TCP) particle tested. CPC 7 [Fig. 1(e)] was noted to be made up of large particle sized microcrystalline HA with the particles exhibiting an angular morphology. CPC 14 [Fig. 1(f)] was observed to be made up of relatively small particle sized amorphous HA with a narrow particle size distribution.

A comparison of the overall shapes of the particles indicated that CPCs 2 and 14 were both small and spherical and CPC 6 was rounded but had an aspect ratio similar to the angular shaped particles, CPC 1, 3, and 7 (Table I). Well plate coverage exceeded 90% in all wells reaching nearly 100% for the small particle CPC 2 and 14 (Table II). Particle surface area varied with larger particles having the highest surface areas exposed to cells.

Cell culture studies

Endothelial cells (MVEC) as a group exhibited a “cobblestone” appearance [Fig. 2(a)] that was previously reported²⁰ and has been noted to be typical of that cell type. Individual cells had stretched processes suggesting spreading and cell adhesion to surfaces [Fig. 2(b)]. BDCs were initially noted to have a trapezoidal shape with a stretched appearance and formed a sheet [Figs. 2(c,d)] as they came to confluence, which was observed in previous studies in which the osteoblast phenotype was confirmed using an alkaline phosphatase assay.²⁵ CDCs [Figs. 2 (e,f)] were also observed to be trapezoidal with a less stretched appearance and assays indicated that they produced proteoglycans as would be expected of chondrocytes.

In the MVEC cultures, cell metabolism (used as an indication of cell numbers) was low on all CPC particle surfaces (Fig. 3). In all wells, MVECs were lost during initial seeding, however reaction to the CPC coatings resulted in an increased cellular metabolic rate ($p < 0.05$ for CPCs 2, 3, 7, and 14) when compared to control wells.

The response of BDCs to the CPC coatings, except for CPC 2, was reduced ($p < 0.05$) compared to the response of cells placed on the epoxy-coated and polystyrene-coated control surfaces (Fig. 3). CPC 2 caused the largest increases in cell metabolism. Other CPCs inhibited BDC proliferation relative to controls.

CDCs exhibited a higher overall metabolism rate. CDCs had the greatest response to CPC 2-coated wells, although the metabolic activity was not statistically significantly different ($p < 0.05$) from the polystyrene controls (Fig. 3).

No significant difference in proliferation was noted between specific cells from different animals. When comparing the MVEC response to the BDC response on the various CPCs, a differential response pattern was noted. BDCs proliferated more rapidly on the epoxy, untreated well surfaces and on CPC 2 in comparison to the MVECs, which proliferated more rapidly on CPC 1, 3, 7, and CPC 14.

A proteoglycan assay, which was used to establish the way that surfaces affected CDCs (Fig. 4), indicated that CDCs produced more sulfated proteoglycan on CPCs by the third week than on control surfaces. After the first week, proteoglycan concentrations in the wells containing CPC 1, 2, and 6 were similar to controls. Proteoglycan production was higher in all wells (for all CPCs) after 2 weeks. At that time point CDCs had produced similar amounts of proteoglycan in wells containing CPCs 1, 2, and 7. The most extensive and consistent levels of proteoglycan production (i.e., showing the least variation after the first week) were noted in wells coated with CPC 2. The greatest variation with time was noted on CPC 7, which had reduced proteoglycan production at the 3-week time point.

DISCUSSION

Rapid, secure attachment of cartilage-covered scaffolds to surrounding tissues is expected to lead to success of implanted tissue engineered constructs. Seeding the surfaces of scaffolds to initiate cartilage tissue formation on one surface of the scaffold and accelerate the rate of bone formation in other locations, as well as induce blood vessel formation within bone forming regions should provide a structure with a region that will heal to existing cartilage and has a separate region of sustained bone formation and maturation. The first step in the development of this process is an understanding of the way in which proliferation of various cell populations can be differentially controlled and guided.

This study is the first in which multiple types of primary cell cultures have been established from the same donor and used to examine the effect of various CPC surfaces on cell proliferation. The proliferation rates of three cell types, on several CPC surfaces were characterized to develop a strategy that could be used to encourage selective growth of each cell and tissue type. The goal of the study was to identify coatings suitable for scaffolds that will eventually be placed within subchondral bone and the articular cartilage of a joint. A CPC coating that encouraged both MVEC and BDC growth was desirable for scaffold segments that will be placed into the subchondral bone region because it will provide a surface that will encourage more rapid bone growth and attachment while providing vascular support to sustain the tissue following *in vivo* placement. A CPC coating that encourages chondrocyte growth while inhibiting MVEC growth is desirable so that scaffold sections in a cartilage defect adjacent to a subchondral scaffold will not develop vasculature. The CPCs used in this study were chosen because they have been extensively characterized as coatings on scaffolds and strain gauges^{21,26,27} One previous experiment in particular, noted that CPC-coated strain gauges that had been cultured with MVECs demonstrated similar accelerated bone attachment *in vivo* to CPC-coated gauges that had protein growth factors applied to their surface.²¹

The current study allowed the characterization of multiple CPC particles so that appropriate combinations of CPCs could be evaluated to begin growing engineered tissues on CPC-coated scaffolds prior to *in vivo* placement. Using different cell types from the same donor is essential as the implants to be used in patients will be seeded with autologous cells. In addition, cells from different donors are likely to have individual specific differences in proliferation rates.

Evaluation of cell number indicated that there was an initial loss of BDCs cultured on all HA surfaces. This drop is in agreement with the work of Sun et al.²⁸ who examined changes in TGF- β 1 and PGE2 concentrations and changes in cell proliferation when HA particles of various sizes derived from the same HA source material were added to osteoblast cultures. In that study, osteoblast growth was initially inhibited in all groups, with the greatest drop in cell population occurring when the smallest particle sized HA was added to the culture. We did not observe a clear correlation between our CPC particle size and BDC population changes. We did note that the smallest particle sized HA showed the least initial loss of cells. This observation in addition to the observation by Sun et al.²⁸ indicates that other properties in combination with particle size affected this initial loss.

Relative to the control and epoxy coated plates all the CPC surfaces, demonstrated higher proliferation rates of MVECs. This is in agreement with published work that demonstrated endothelial cells proliferate and maintain their phenotype when cultured with hydroxyapatite.²⁹ In that study HA was found to have no cytotoxic effect on endothelial cells and the cells exposed to HA had higher levels of eNOS in their cytoplasm.²⁹ The results of our study demonstrate that the effectiveness of many types of CPC particles with varying physical and chemical properties to support MVEC growth. The proliferation of MVECs on CPC surfaces and the maintenance of their phenotype²⁹ may explain why CPC-coated implants cultured with MVECs have previously demonstrated rapid bone attachment following *in vivo* placement.²¹ Taking into consideration previous studies³⁰ in which implants coated with CPC 7 encouraged rapid and secure bone attachment (showing bond strengths of 4.8 MPa in 6 weeks), this study supports the use of CPC 7 if MVECs are to be grown on the CPC surface in culture for placement in a bone bed *in vivo*.

The results of this current study demonstrate that CPC coatings and epoxy without embedded CPC particles may be used to selectively control MVEC and BDC growth on segments of a scaffold. This is because MVEC proliferation is inhibited on epoxy-coated surfaces relative to BDC proliferation. Therefore, epoxy without embedded CPC particles can be used to encourage BDC attachment and CPC coatings can be used to guide MVEC growth. CPC 7 would be ideal to segregate the BDC and MVEC population *in vitro*, as BDC growth is inhibited relative to MVEC growth on these surfaces.

Growth of CDCs (relative to controls) was also inhibited in the presence of most CPCs. One exception was that CDCs exhibited extensive cell proliferation on CPC 2 particles. The proliferation of CDCs on CPC 2 was not statistically significantly different ($p < 0.05$) from the control or epoxy coated wells, however measurement of proteoglycan production by the cultured cells indicated that the cells maintained their phenotype on the CPC 2 surface and produced proteoglycan while they did not in control wells. In addition to supporting CDC growth and maintaining chondrocyte phenotype, the growth rate of MVECs in particular were significantly lower on the CPC 2 coated wells. This demonstrated that small particle sized, spherical, crystalline, CPC 2 is the best surface coating to use in future experiments to quickly expand the cell population and maintain cell phenotype for CDCs while cartilage tissue is grown *in vitro*.

In general, the results of this experiment indicate that CDCs can maintain their phenotype when cultured on CPC surfaces, as all the CDCs cultured on CPC-coated wells produced more proteoglycan by the second and third weeks of the experiment when compared to control wells. This result is in agreement with a study performed by Ciolfi et al.³¹ that demonstrated chondrocytes cultured on a calcium phosphate surface can maintain their phenotype and produce cartilage-like matrix *in vitro*. In addition *in vivo* studies conducted by Tanaka et al.³² demonstrated a biphasic scaffold with a CPC base can maintain the phenotype of chondrocytes suspended in a collagen gel and seeded on the surface of the implant following

placement into a knee joint. The peak concentration of proteoglycan in our experiments occurred after being cultured on the CPC surfaces for 3 weeks. However, the Tukey HSD test indicated that 3-week culture results were not statistically significantly different than the 2-week results. Even though there were no significant differences, the patterns also suggested that CPCs began to dedifferentiate on CPC 7 at the 3-week time point.

Numerous cell culture studies have indicated that surface topography may be more important than surface chemistry in regulating the cell growth and maintenance of phenotype. One recently study by Rea et al.³³ noted a difference in osteoblast differentiation and proliferation on various surface topographies and observed no correlation between surface chemistry, and differentiation and proliferation. Earlier studies by Martin et al.,³⁴ who examined the effect of surface roughness on human osteoblast proliferation, differentiation, and protein synthesis, noted that thymidine incorporation and alkaline phosphatase activity were inversely related to surface roughness while proteoglycan synthesis was inhibited on all rough surfaces. Endothelial cells have been noted to have a similar dependence on surface topographies as was noted in studies that looked at pore size and spacing,²⁹ as well as surface roughness.³⁰ The results of this experiment are consistent with previous experiments²⁸ showing inhibited osteoblast growth on relatively rougher surfaces. However, the increased MVEC proliferation noted on CPC surfaces in this study conflicts with a previous study demonstrating endothelial cells preferred smooth surfaces,³⁰ since the CPC particle coatings have much more surface roughness than the control and epoxy coated wells where MVEC proliferation was inhibited to a greater extent. One limitation of this current study is the CPC particles used did not allow for clear separation of size, shape, and crystalline structure into independent variables between different CPC types. As such no clear conclusions can be made regarding the relative importance of these variables on these CPC surfaces. Despite this limitation, our observations do suggest no correlation between cell growth and these individual variables, suggesting rather that a combination of factors may be synergistic in determining cell proliferation and that one single variable may not adequately explain cell proliferation differences.

The goal of this experiment was to identify CPC surfaces that would encourage bone and vascular cell growth on one CPC-coated surface, and would support chondrocyte growth on another type of CPC-coated surface while inhibiting the proliferation of MVECs. Separation of BDCs and MVECs on a CPC-coated implant would be best achieved using epoxy without embedded CPC to encourage BDC growth, and use of CPC 3 or 14 to encourage MVEC growth and inhibit BDC growth. The relatively high rate of MVEC proliferation on CPC 7, and previous experiments demonstrating that MVECs cultured on CPC surfaces accelerates bone attachment *in vivo* on CPC 7 surfaces,²¹ and the fact that even CPC 7 alone supports rapid *in vivo* bone attachment,²¹ indicate that the CPC 7 coating is ideal for bone bonding implants that have MVECs grown on them prior to *in vivo* placement while CPC 2 clearly provided the best surface for chondrocyte proliferation. In addition chondrocytes cultured on this CPC surface maintained their phenotypes.

References

1. Arthritis Foundation. Conditions and Treatments; Disease Center; OA—Overview. [Accessed October 2005]. Available at http://www.arthritis.org/conditions/DiseaseCenter/OA/oa_overview.asp
2. Chen FS, Frenkel SR, Di Cesare PE. Repair of articular cartilage defects: Part II. Treatment options Am J Orthop 1999;28:88–96.
3. Hunziker EB. Articular cartilage repair: Are the intrinsic biological constraints undermining this process insuperable? Osteoarthritis Cartilage 1999;7:15–28. [PubMed: 10367012]
4. Woodfield TB, Bezemer JM, Pieper JS, van Blitterswijk CA, Riesle J. Scaffolds for tissue engineering of cartilage. Crit Rev Eukaryot Gene Expr 2002;12:209–236. [PubMed: 12449344]

5. Barrack RL, Skinner HB, Cook SD, Haddad RJ Jr. Effect of articular disease and total knee arthroplasty on knee joint-position sense. *J Neurophysiol* 1983;50:684–687. [PubMed: 6619913]
6. Lavernia, C.; Guzman, J.; Kabo, M.; Krakow, K.; Hungerford, D. Polyethylene wear in autopsy retrieved fully functional total knee replacement. Sixtieth Meeting of the American Academy of Orthopedic Surgeons; 2000. p. 273
7. Han CD, Choe WS, Yoo JH. Effect of polyethylene wear on osteolysis in cementless primary total hip arthroplasty: Minimal 5-year follow-up study. *J Arthroplasty* 1999;14:714–723. [PubMed: 10512444]
8. Caplan AI, Elyaderani M, Mochizuki Y, Wakitani S, Goldberg VM. Principles of cartilage repair and regeneration. *Clin Orthop Relat Res* 1997;342:254–269. [PubMed: 9308548]
9. Reddi AH. Morphogenesis and tissue engineering of bone and cartilage: Inductive signals, stem cells, and biomimetic biomaterials. *Tissue Eng* 2000;6:351–359. [PubMed: 10992432]
10. Temenoff JS, Mikos AG. Review: Tissue engineering for regeneration of articular cartilage. *Biomaterials* 2000;21:431–440. [PubMed: 10674807]
11. Yamaguchi M, Shinbo T, Kanamori T, Wang PC, Niwa M, Kawakami H, Nagaoka S, Hirakawa K, Kamiya M. Surface modification of poly(L-lactic acid) affects initial cell attachment, cell morphology, and cell growth. *J Artif Organs* 2004;7:187–193. [PubMed: 15739051]
12. Cronin EM, Thurmond FA, Bassel-Duby R, Williams RS, Wright WE, Nelson KD, Garner HR. Protein-coated poly(L-lactic acid) fibers provide a substrate for differentiation of human skeletal muscle cells. *J Biomed Mater Res* 2004;69:373–381.
13. Mann BK, West JL. Cell adhesion peptides alter smooth muscle cell adhesion, proliferation, migration, and matrix protein synthesis on modified surfaces and in polymer scaffolds. *J Biomed Mater Res* 2002;60:86–93. [PubMed: 11835163]
14. Berry CC, Campbell G, Spadicino A, Robertson M, Curtis AS. The influence of microscale topography on fibroblast attachment and motility. *Biomaterials* 2004;25:5781–5788. [PubMed: 15147824]
15. Tan J, Shen H, Saltzman WM. Micron-scale positioning of features influences the rate of polymorphonuclear leukocyte migration. *Biophys J* 2001;81:2569–2579. [PubMed: 11606271]
16. Wan Y, Wang Y, Liu Z, Qu X, Han B, Bei J, Wang S. Adhesion and proliferation of OCT-1 osteoblast-like cells on micro- and nano-scale topography structured poly(L-lactide). *Biomaterials* 2005;26:4453–4459. [PubMed: 15701374]
17. Ishaug SL, Crane GM, Miller MJ, Yasko AW, Yaszemski MJ, Mikos AG. Bone formation by three-dimensional stromal osteoblast culture in biodegradable polymer scaffolds. *J Biomed Mater Res* 1997;36:17–28. [PubMed: 9212385]
18. Boby JD, Pilliar RM, Cameron HU, Weatherly GC. The optimum pore size for the fixation of porous-surfaced metal implants by the ingrowth of bone. *Clin Orthop Relat Res* 1980;150:263–270. [PubMed: 7428231]
19. Szivek JA, Margolis DS, Garrison BK, Nelson E, Vaidyanathan RK, DeYoung DW. TGF- β 1-enhanced TCP-coated sensate scaffolds can detect bone bonding. *J Biomed Mater Res B Appl Biomater* 2005;73:43–53. [PubMed: 15682399]
20. Szivek, JA.; Williams, SK.; Cordaro, JM.; Mermelstein, R.; Neville, R. In Vitro Performance of CPC Coatings Used to Bond Strain Gauges to Bone. Scottsdale, AZ: Surfaces in Biomaterials; 2000. p. 228-231.
21. Szivek JA, Anderson PL, Dishongh TJ, DeYoung DW. Evaluation of factors affecting bonding rate of calcium phosphate ceramic coatings for in vivo strain gauge attachment. *J Biomed Mater Res* 1996;33:121–132. [PubMed: 8864883]
22. Williams SK, Jarrell BE, Rose DG, Pontell J, Kapelan BA, Park PK, Carter TL. Human microvessel endothelial cell isolation and vascular graft sodding in the operating room. *Ann Vasc Surg* 1989;3:146–152. [PubMed: 2765356]
23. Jarrell B, Levine E, Shapiro S, Williams S, Carabasi RA, Mueller S, Thornton S. Human adult endothelial cell growth in culture. *J Vasc Surg* 1984;1:757–764. [PubMed: 6436516]
24. Farndale RW, Buttle DJ, Barrett AJ. Improved quantitation and discrimination of sulphated glycosaminoglycans by use of dimethylmethylene blue. *Biochim Biophys Acta* 1986;883:173–177. [PubMed: 3091074]

25. Fernandes, MM.; Szivek, JA.; Grana, WA.; Margolis, DS.; Blumenkron, F.; Calvert, PD.; Bourque, PP.; Vaidyanathan, R.; Hoying, JB. Preliminary Tissue Engineering Studies of Cartilage/Bone Composites for Joint Resurfacing. Scottsdale, AZ: Surfaces in Biomaterials; 2002. p. 20
26. Maliniack MM, Szivek JA, DeYoung DW. The development of hydroxyapatite coated strain gauges for long-term in vivo bone loading response measurements. *J Appl Biomater* 1993;4:143–152. [PubMed: 10171661]
27. Szivek JA, Bliss CL, Geffre CP, Margolis DW, DeYoung DW, Ruth AB, Schnepf AB, Tellis BC, Vaidyanathan RK. An instrumented scaffold can monitor loading in the knee joint. *J Biomed Mater Res B Appl Biomater* 2006;79:218–228. [PubMed: 16637034]
28. Sun JS, Liu HC, Chang WH, Li J, Lin FH, Tai HC. Influence of hydroxyapatite particle size on bone cell activities: An in vitro study. *J Biomed Mater Res* 1998;39:390–397. [PubMed: 9468047]
29. Pezzatini S, Solito R, Morbidelli L, Boanini E, Bigi A, Ziche M. The effect of hydroxyapatite nanocrystals on microvascular endothelial cell viability and functions. *J Biomed Mater Res* 2006;76:656–663.
30. Battraw GA, Szivek JA, Anderson PL. Bone bonding strength of calcium phosphate ceramic coated strain gauges. *J Biomed Mater Res B Appl Biomater* 1999;48:32–35.
31. Ciolfi VJ, Pilliar R, McCulloch C, Wang SX, Grynblas MD, Kandel RA. Chondrocyte interactions with porous titanium alloy and calcium polyphosphate substrates. *Biomaterials* 2003;24:4761–4770. [PubMed: 14530073]
32. Tanaka T, Komaki H, Chazono M, Fujii K. Use of a biphasic graft constructed with chondrocytes overlying a β -tricalcium phosphate block in the treatment of rabbit osteochondral defects. *Tissue Eng* 2005;11:331–339. [PubMed: 15738686]
33. Rea SM, Brooks RA, Schneider A, Best SM, Bonfield W. Osteoblast-like cell response to bioactive composites-surface-topography and composition effects. *J Biomed Mater Res B Appl Biomater* 2004;70:250–261. [PubMed: 15264307]
34. Martin JY, Schwartz Z, Hummert TW, Schraub DM, Simpson J, Lankford J Jr, Dean DD, Cochran DL, Boyan BD. Effect of titanium surface roughness on proliferation, differentiation, and protein synthesis of human osteoblast-like cells (MG63). *J Biomed Mater Res* 1995;29:389–401. [PubMed: 7542245]

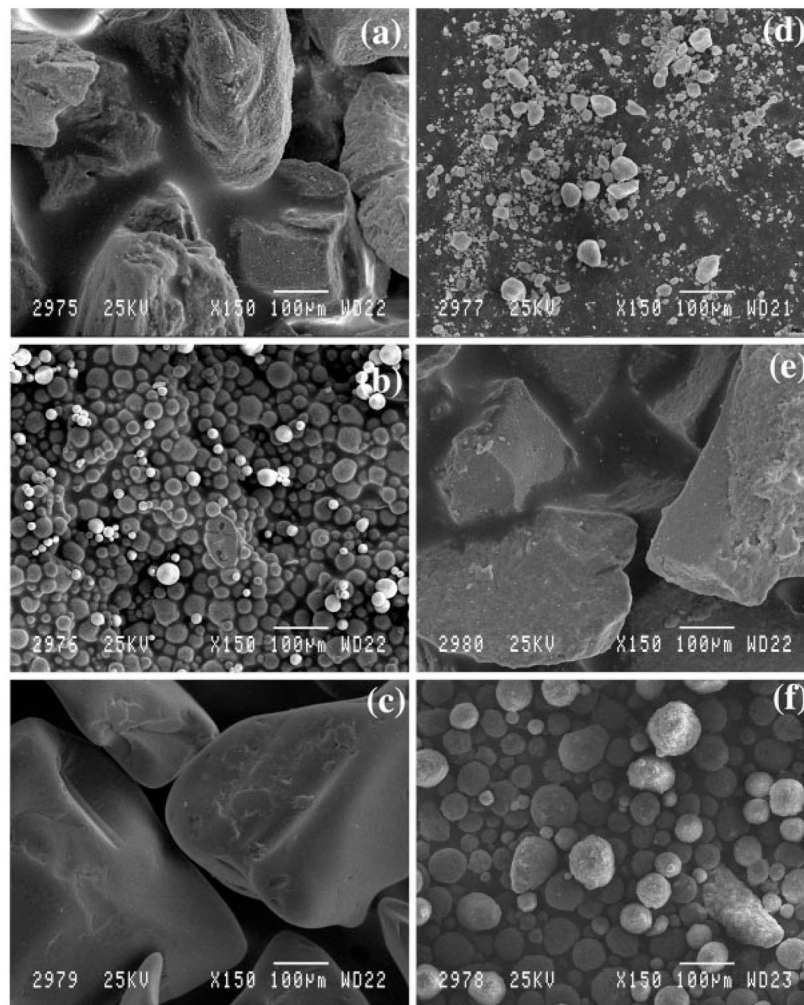


Figure 1.

This collage of scanning electron micrographs shows (a) CPC 1. These particles were angular with a high degree of surface roughness and XRD indicated that they were a relatively crystalline hydroxyapatite. (b) CPC 2. These particles were observed to be spherical and XRD indicated that they were a relatively crystalline hydroxyapatite. (c) CPC 3. These particles were large and angular and XRD indicated that they were a relatively amorphous hydroxyapatite. (d) CPC 6. These particles were observed to be rounded and XRD indicated that they were a relatively amorphous tri-calcium phosphate. (e) CPC 7. These particles were noted to be very large and angular and XRD indicated that they were a highly crystalline hydroxyapatite with a small grain size. (f) CPC 14. These particles were rounded but larger than the CPC 6 particles and XRD indicated that they were a relatively amorphous hydroxyapatite. Table II provides the coverage ratios for wells coated with each type of CPC.

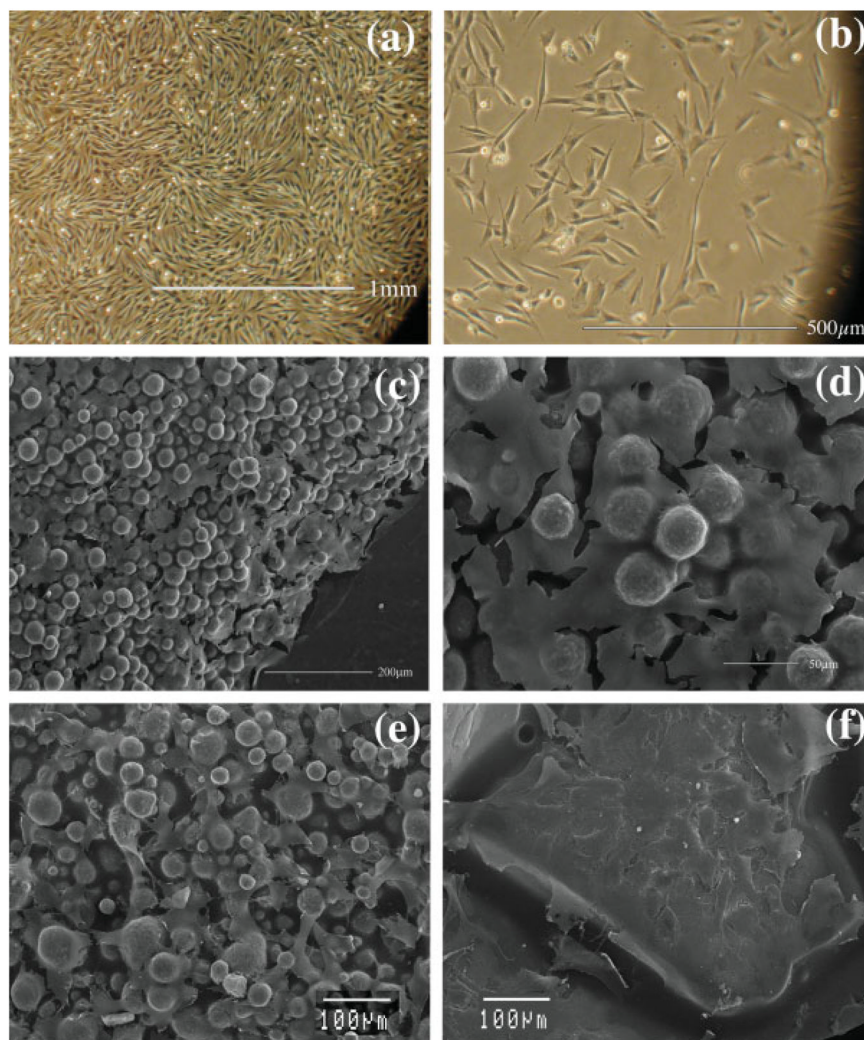


Figure 2.

This collage of pictures shows (a) pictures taken with an inverted microscope showing MVECs in culture dishes at 100 \times . (b) Picture taken with an inverted microscope showing MVECs in culture dishes at 200 \times . (c) A scanning electron micrograph taken at 150 \times magnification shows a continuous layer of BDCs on a CPC surface. (d) A scanning electron micrograph taken at 450 \times magnification shows a higher magnification view of the continuous layer of BDCs on a CPC surface. (e) A scanning electron micrograph taken at 300 \times shows CDCs on the small particle sized CPC 2. (f) A scanning electron micrograph taken at 300 \times shows CDCs on the large particle sized CPC 3. [Color figure can be viewed in the online issue, which is available at www.interscience.wiley.com.]

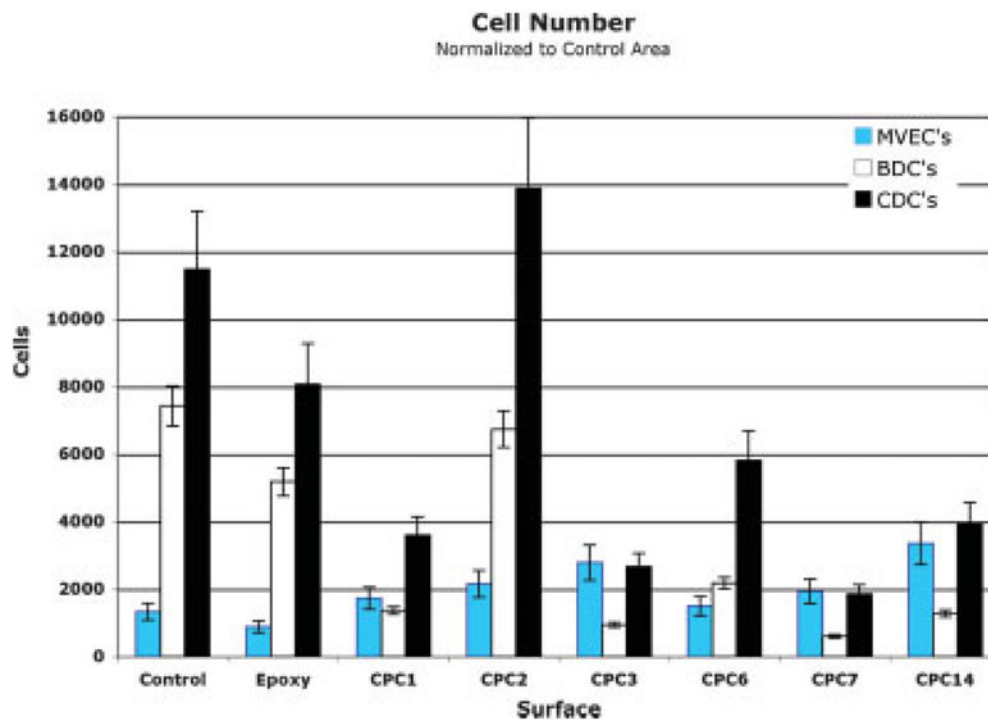


Figure 3.

This chart shows a comparison of the proliferation of CDCs and BDCs with MVECs. Based on this comparison, selection of a CPC 2 coating to guide CDCs and a CPC 3, 7 or CPC 14 coating to guide MVECs would be expected to provide rapid proliferation of these cell types in specifically defined locations. This graph also indicates that MVECs proliferated relatively poorly on epoxy, CPC 2, and CPC 6 and BDCs proliferate best on epoxy. Thirty wells coated with each CPC surface were evaluated for each cell type to create this graph. [Color figure can be viewed in the online issue, which is available at www.interscience.wiley.com.]

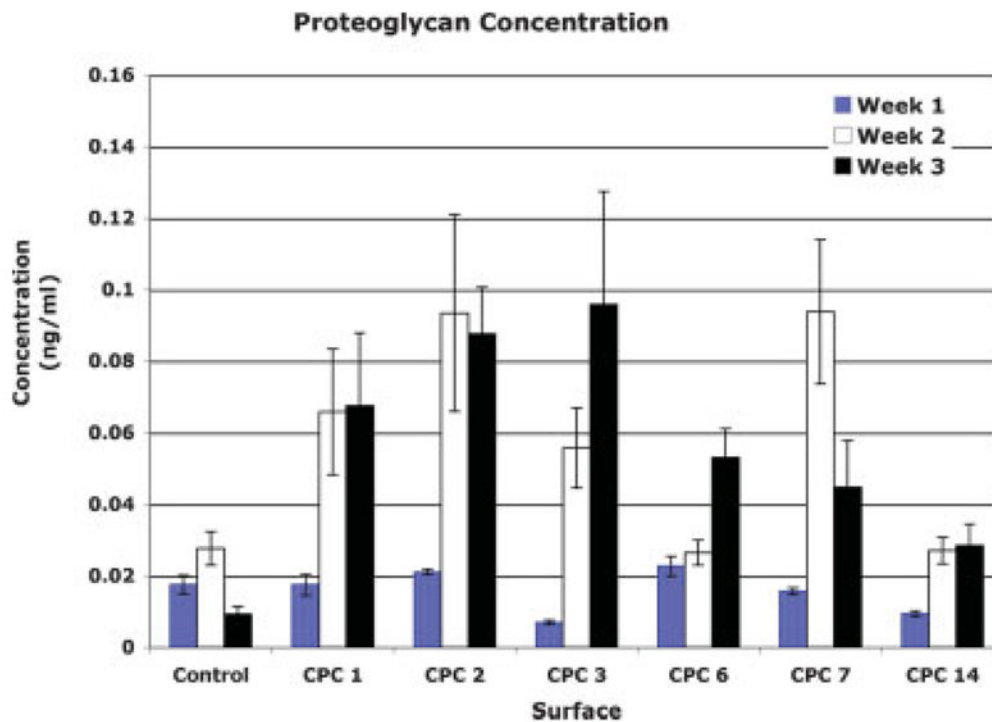


Figure 4.

A comparison of the proteoglycan production in wells coated with CPCs after 1, 2, and 3 weeks. Although no statistically significant difference in concentration was found for surfaces between week 2 and 3, there was a clear trend showing a reduction in proteoglycan concentration on CPC 7. Eighteen wells coated with each surface were evaluated at each time point to create this graph. [Color figure can be viewed in the online issue, which is available at www.interscience.wiley.com.]

TABLE I

CPC Particle Characteristics

CPC	Shape	Crystallinity and Material	Particle Size Range (μm , min \pm std dev to max \pm std dev)
1	Angular	Crystalline HA	103 \pm 62 to 197 \pm 114
2	Spherical	Crystalline HA	16 \pm 8 dia.
3	Angular	Amorphous HA	88 \pm 43 to 184 \pm 95
6	Spherical	Amorphous TCP	6 \pm 5 to 9 \pm 7
7	Angular	Microcrystalline HA	515 \pm 164 to 561 \pm 85
14	Spherical	Amorphous HA	40 \pm 12 dia.

TABLE II
Surface Area and Percent Surface Coverage of Well Plates

CPC Type	Surface Area (mm ²)	% Surface Covered with CPC
Control	54.4 ± 0.3	0.0 ± 0.0
Epoxy	86.2 ± 0.3	0.0 ± 0.0
1	165.2 ± 0.1	94.1 ± 2.1
2	86.0 ± 0.3	99.4 ± 1.0
3	128.0 ± 0.3	95.4 ± 2.5
6	94.8 ± 0.5	98.2 ± 2.9
7	195.4 ± 0.2	90.2 ± 3.4
14	87.3 ± 0.0	99.2 ± 1.4